

# The regulatory domain of protein kinase C $\theta$ localises to the Golgi complex and induces apoptosis in neuroblastoma and Jurkat cells

A Schultz<sup>1</sup>, J-I Jönsson<sup>1</sup> and C Larsson<sup>\*1</sup>

<sup>1</sup> Lund University, Molecular Medicine, Entrance 78, 3rd floor, UMAS, 205 02 Malmö, Sweden

\* Corresponding author: C Larsson. Tel: +46-40-337404; Fax: +46-40-337322; E-mail: Christer.Larsson@molmed.mas.lu.se

Received 6.8.02; revised 17.1.03; accepted 24.1.03  
Edited by JA Cidlowski

## Abstract

This study investigates apoptotic effects of protein kinase C (PKC)  $\delta$  and  $\theta$  in neuroblastoma cells. 12-*O*-tetradecanoylphorbol-13-acetate induces apoptosis in SK-N-BE(2) neuroblastoma cells overexpressing PKC $\delta$  or PKC $\theta$ , but not PKC $\epsilon$ . The PKC inhibitor GF109203X does not suppress this apoptotic effect, suggesting that it is independent of the catalytic activity of PKC. The isolated catalytic domains of PKC $\delta$  and PKC $\theta$  or the regulatory domain (RD) of PKC $\theta$  also induce apoptosis in neuroblastoma cells. The apoptotic responses are suppressed by caspase inhibition and by Bcl-2 overexpression. The PKC $\theta$  RD induced apoptosis also in Jurkat cells. Colocalisation analysis revealed that the PKC $\theta$  RD primarily localises to the Golgi complex. The C1b domain is required for this localisation and removal of the C1b domain results in a PKC $\theta$  construct that does not induce apoptosis. This suggests that the PKC $\theta$  RD has apoptotic activity and that Golgi localisation may be important for this effect.

*Cell Death and Differentiation* (2003) 10, 662–675. doi:10.1038/sj.cdd.4401235

**Keywords:** protein kinase C; C1 domain; apoptosis; Golgi apparatus; neuroblastoma; Jurkat

**Abbreviations:** CD, catalytic domain; EGFP, enhanced green fluorescent protein; PKC, protein kinase C; TPA, 12-*O*-tetradecanoylphorbol-13-acetate; RD, regulatory domain.

## Introduction

Apoptosis, programmed cell death, is critical for the removal of unwanted cells during the development and life of multicellular organisms. The importance of this process is illustrated by the fact that a decreased capacity to enter apoptosis is common to most, if not all, cancer cells. The regulation of apoptosis is complex and involves a multitude of signalling pathways. A number of studies have shown that different protein kinase C

(PKC) isoforms play important roles both in supporting cell survival and in facilitating the induction of apoptosis. The PKC family comprises at least 10 different isoforms of phospholipid-dependent serine/threonine kinases divided into three subgroups depending on their structure and requirements for activation. The classical PKCs ( $\alpha$ ,  $\beta$ I,  $\beta$ II and  $\gamma$ ) are Ca<sup>2+</sup>-dependent and activated by diacylglycerol and phorbol esters. Novel PKCs ( $\delta$ ,  $\epsilon$ ,  $\eta$  and  $\theta$ ) are also activated by diacylglycerol and phorbol esters but they are insensitive to Ca<sup>2+</sup>, whereas atypical PKCs ( $\zeta$  and  $\iota$ ) are insensitive to Ca<sup>2+</sup> as well as diacylglycerol and phorbol esters.

The basic structure of PKC is a single polypeptide chain with an NH<sub>2</sub>-terminal regulatory domain (RD) and a COOH-terminal catalytic domain (CD). The RD of the classical and novel PKCs contains two classes of domains, C1 and C2, which bind PKC activators. Diacylglycerol and phorbol esters bind to the C1 domains and Ca<sup>2+</sup> binds to the C2 domain of classical isoforms.<sup>1–3</sup>

So far, no general pattern of the role of PKC isoforms in apoptosis has emerged. Instead, the same PKC isoform can have both pro- and antiapoptotic effects depending on the cell type. However, accumulating data indicate that the novel PKC $\delta$  isoform is involved in the onset of apoptosis induced by a wide range of stimuli. These include Fas ligand,<sup>4</sup> reactive oxygen species,<sup>5</sup> hyperglycaemia<sup>6</sup> and DNA-damaging agents like UV irradiation<sup>7</sup> and etoposide.<sup>8</sup> PKC $\delta$  has been shown to influence different steps in apoptotic pathways such as generation of ceramide,<sup>9</sup> alteration of the mitochondrial membrane potential<sup>10</sup> and the activation of caspases.<sup>8</sup> Furthermore, PKC $\delta$ <sup>4,7,8,11–13</sup> and the novel isoforms PKC $\epsilon$ <sup>4</sup> and PKC $\theta$ <sup>4,14</sup> are cleaved by caspases, and this leads to the generation of free CDs and RDs. The importance of this is substantiated by the finding that expression of PKC $\delta$ CD<sup>4,12,15</sup> or PKC $\theta$ CD<sup>14</sup> induces apoptosis. However, both PKC $\epsilon$ <sup>16,17</sup> and PKC $\theta$ <sup>16,18</sup> have also been suggested to protect against apoptotic insults.

The general role of classical PKC isoforms in the regulation of apoptosis is also indistinct. PKC $\alpha$  for instance has been reported to suppress apoptosis in Cos cells<sup>19</sup> and to enhance the phosphorylation and possibly the activation of Bcl-2.<sup>20</sup> Furthermore, a classical isoform counteracts Fas-induced apoptosis in Jurkat cells.<sup>21</sup> On the other hand, activation of PKC $\alpha$  leads to apoptosis in LNCaP cells.<sup>22,23</sup>

Neuroblastoma is the most common extracranial solid tumour affecting children. In many cases, these tumours are highly malignant and frequently recur with a multidrug-resistant phenotype, which renders them incurable. It is therefore necessary to find novel means to block the growth of these cells. This study was designed to investigate whether novel PKC isoforms have proapoptotic effects in neuroblastoma cells. The results demonstrate that treatment with a

PKC-activating phorbol ester induces apoptosis in SK-N-BE(2) neuroblastoma cells that overexpress the novel PKC isoforms  $\delta$  and  $\theta$ , independently of the kinase activity of PKC. Furthermore, it is shown that the isolated RD of PKC $\theta$  by itself induces apoptosis and this effect is correlated to a localisation to the Golgi apparatus, which is mediated by the C1b domain of the protein.

## Results

### TPA treatment leads to apoptosis in SK-N-BE(2) cells overexpressing the novel PKC isoforms $\delta$ or $\theta$ , but not $\epsilon$

To investigate whether novel PKC isoforms are proapoptotic in neuroblastoma cells, the malignant and multidrug-resistant SK-N-BE(2) neuroblastoma cell line was transfected with expression vectors encoding full-length PKC $\delta$ , PKC $\epsilon$  or PKC $\theta$  fused to enhanced green fluorescent protein (EGFP), or an expression vector encoding EGFP alone. After transfection, cells were grown in the absence or presence of 16 nM of the PKC activator 12-*O*-tetradecanoylphorbol-13-acetate (TPA) and/or 2  $\mu$ M of the PKC inhibitor GF109203X for 16 h. Apoptosis was analysed by staining the nuclei with propidium iodide and checking for condensed and fragmented nuclei (Figure 1). The experiment revealed that neither treatment with TPA, GF109203X nor the combination of them had an apoptosis-inducing effect in cells expressing EGFP alone (Figure 1a). However, upon addition of TPA, 6.8% of the cells

overexpressing PKC $\delta$  were apoptotic, compared to 3.8% after treatment with vehicle (Figure 1b). A similar but more pronounced effect was seen in PKC $\theta$ -overexpressing cells, in which TPA treatment led to apoptosis in 9.4% of the cells compared to 2.8% in untreated cells (Figure 1d). To investigate whether the effect is dependent on the catalytic activity of PKC, the PKC inhibitor GF109203X was included concomitantly with TPA. The inhibitor did not suppress the effect of TPA in cells overexpressing PKC $\delta$  or PKC $\theta$ . Instead, GF109203X further potentiated the TPA induction of apoptosis and the effect was most prominent in cells overexpressing PKC $\delta$ -EGFP. Treatment with GF109203X alone did not lead to apoptosis. This suggests that apoptosis induced by TPA treatment in cells overexpressing PKC $\delta$  or PKC $\theta$  is independent of the kinase activity of the enzyme. In contrast, cells overexpressing PKC $\epsilon$  were neither influenced by TPA treatment alone, nor by the combined treatment of TPA and GF109203X (Figure 1c).

### Effects of isolated catalytic and regulatory PKC domains on apoptosis

In several cell systems, PKC $\delta$  and PKC $\theta$  are proteolytically cleaved by caspases during apoptosis.<sup>4,12,14</sup> This leads to the generation of free CDs and RDs. To analyse whether the free CD can induce apoptosis, vectors encoding PKC $\delta$ CD, PKC $\epsilon$ CD or PKC $\theta$ CD fused to EGFP or the empty EGFP vector were transfected into SK-N-BE(2) cells. Transfected cells were scored for apoptosis based on the morphology of the nuclei, visualised by staining with propidium iodide. Both PKC $\delta$ CD and PKC $\theta$ CD expression induced a higher rate of apoptosis compared to control-transfected neuroblastoma cells, whereas PKC $\epsilon$ CD expression had no major effect (Figure 2a).

To confirm that apoptosis provoked by PKC $\delta$ CD and PKC $\theta$ CD is dependent on the kinase activity, SK-N-BE(2) cells expressing PKC $\delta$ CD or PKC $\theta$ CD were treated with GF109203X. This inhibitor reduced the rate of apoptosis from 9.7 to 5.7% in cells expressing PKC $\delta$ CD and from 14.5 to 4.8% in cells expressing PKC $\theta$ CD. GF109203X did not affect the level of apoptosis in cells expressing EGFP alone (Figure 2b).

To assess whether overexpression of the RDs of PKC also induces apoptosis, SK-N-BE(2) cells were transfected with vectors encoding PKC $\alpha$ RD, PKC $\beta$ RD, PKC $\delta$ RD, PKC $\epsilon$ RD, PKC $\eta$ RD or PKC $\theta$ RD fused to EGFP or the empty EGFP vector (Figure 2c). There was a tendency to higher levels of apoptosis upon overexpression of either of these RDs. The largest effect was observed in cells transfected with the PKC $\theta$ RD vector. To exclude that the apoptotic effect of  $\theta$ RD is because of a higher expression level, SK-N-BE(2) cells were transfected with vectors encoding the different RDs and subjected to a Western blot analysis using an EGFP antibody (Figure 2c). This clearly demonstrates that PKC $\theta$ RD together with PKC $\eta$ RD are expressed at the lowest levels, which confirms that the larger apoptotic effect of PKC $\theta$ RD is not because of it being expressed at higher levels than other RDs. Expression of PKC $\theta$ RD also induced apoptosis in two other neuroblastoma cell lines, KCN-69n and SK-N-SH,

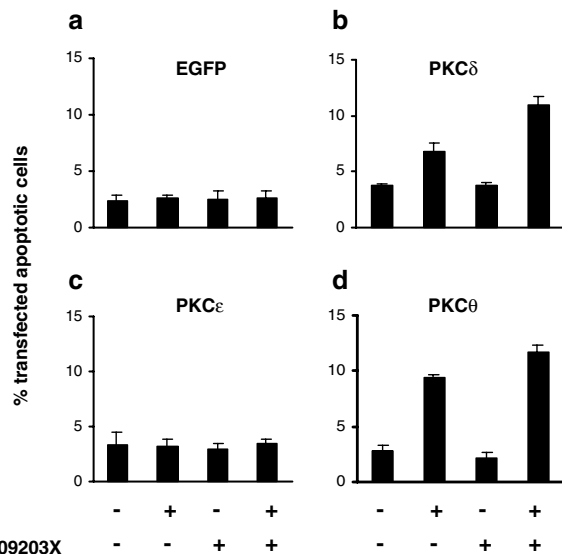


**Figure 1** TPA treatment leads to apoptosis in SK-N-BE(2) cells overexpressing the novel PKC isoforms  $\delta$  or  $\theta$ , but not  $\epsilon$ . SK-N-BE(2) neuroblastoma cells were transfected with vectors encoding EGFP (a) or PKC $\delta$  (b), PKC $\epsilon$  (c) or PKC $\theta$  (d) fused to EGFP. After transfection, 16 nM TPA and/or 2  $\mu$ M GF109203X were added to the cell medium in combinations indicated in the figure. Cells were fixed and nuclei were stained with propidium iodide 16 h after transfection. Transfected cells were visualised by the fluorescence of EGFP and apoptotic cells were quantified based on nuclear morphology. Data (mean  $\pm$  S.E.M.,  $n=3$ ) are presented as percent transfected cells with apoptotic nuclei

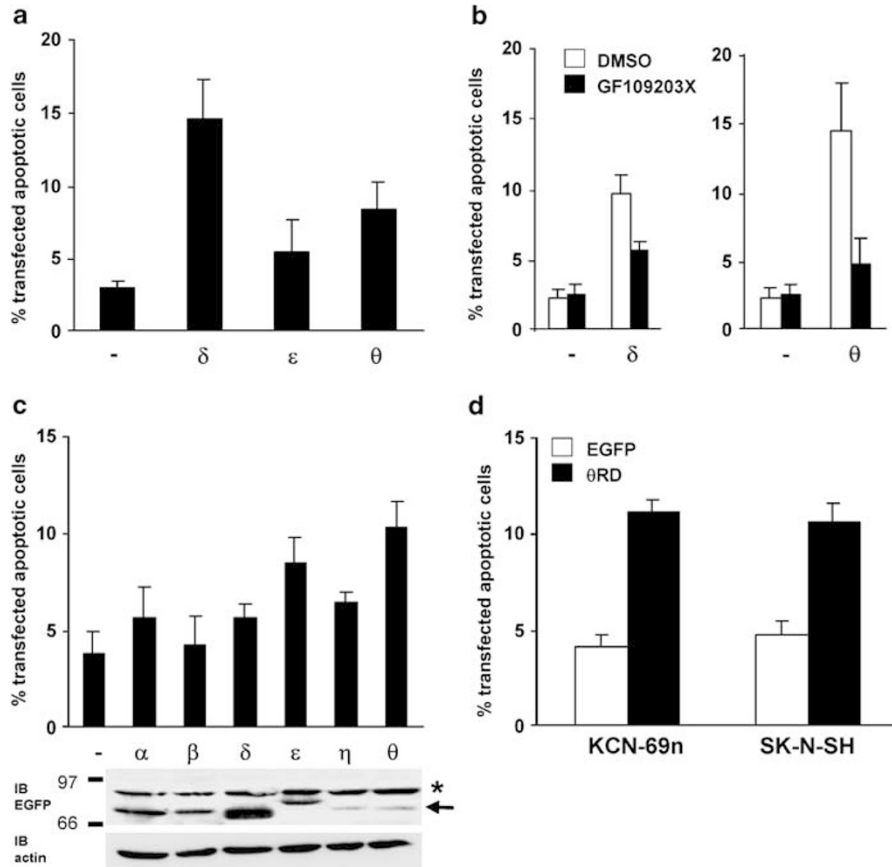


**Figure 2** Apoptotic effects of isolated PKC CDs and RDs. (a) SK-N-BE(2) neuroblastoma cells were transfected with expression vectors encoding EGFP (–) or CDs of PKC $\delta$  ( $\delta$ ), PKC $\epsilon$  ( $\epsilon$ ) or PKC $\theta$  ( $\theta$ ) fused to EGFP. (b) SK-N-BE(2) neuroblastoma cells transfected with an EGFP vector (–) or vectors encoding the CDs of PKC $\delta$  ( $\delta$ ) or PKC $\theta$  ( $\theta$ ) fused to EGFP were treated with 2  $\mu$ M GF109203X or vehicle (DMSO) after the end of transfection. (c) SK-N-BE(2) cells were transfected with expression vectors encoding EGFP (–) or the RDs of PKC $\alpha$  ( $\alpha$ ), PKC $\beta$  ( $\beta$ ), PKC $\delta$  ( $\delta$ ), PKC $\epsilon$  ( $\epsilon$ ), PKC $\eta$  ( $\eta$ ) or PKC $\theta$  ( $\theta$ ) fused to EGFP. (d) SK-N-SH or KCN-69n neuroblastoma cells were transfected with expression vectors encoding EGFP or the RD of PKC $\theta$  ( $\theta$ RD). Cells were in all experiments fixed 16 h after transfection and nuclei were stained with propidium iodide. Transfected cells were visualised by the fluorescence of EGFP and scored for apoptotic morphology. Data (mean  $\pm$  S.E.M.,  $n=3$ ) are presented as percent transfected cells with apoptotic nuclei. The Western blots in (c) demonstrate expression levels of the different EGFP fusion proteins (upper panel, analysed with an anti-EGFP antibody) and actin as a loading control (lower panel). Positions of the weight markers 97 and 66 kDa are shown to the left of the EGFP blot. The arrow indicates reactivity corresponding to PKC–EGFP fusion proteins and the star denotes an unspecific band

demonstrating that the apoptotic effect is not limited to one specific cell line (Figure 2d). Thus, not only free PKC $\delta$  and PKC $\theta$  CDs, but also the PKC $\theta$ RD is apoptotic in neuroblastoma cells.

### Inhibition of the apoptotic effects of PKC $\delta$ and PKC $\theta$ by Bcl-2 overexpression and a caspase-inhibitor

The family of antiapoptotic Bcl-2 proteins play important roles in the regulation of the mitochondrial pathway of apoptosis, a process that eventually leads to activation of caspase-3 (reviewed in Hengartner<sup>24</sup>). We therefore investigated whether Bcl-2 overexpression or caspase inhibition could protect against induction of apoptosis by expression of PKC $\delta$ CD, PKC $\theta$ RD or by TPA treatment of cells overexpressing full-length PKC $\delta$  or PKC $\theta$ . Cotransfection with a Bcl-2 vector resulted in a substantial reduction of the rate of apoptosis induced by expression of either PKC $\delta$ CD or

PKC $\theta$ RD (Figure 3a). Bcl-2 also suppressed the apoptosis induced by TPA treatment of SK-N-BE(2) cells overexpressing full-length PKC $\delta$  or PKC $\theta$  (Figure 3b). Expression of Bcl-2 resulted in rates of apoptosis similar to what was seen in cells overexpressing PKC $\delta$  or PKC $\theta$  that were not exposed to TPA. The generation of Bcl-2 protein by the expression vector was confirmed by transfecting SK-N-BE(2) cells with the vector and analysing cell lysates with Western blot using an antibody towards Bcl-2 (Figure 3c). It should be noted that, although it is not evident in the figure, a weak band corresponding to endogenously expressed Bcl-2 could be detected after long exposure of the blot (not shown). A reduction of the rate of apoptotic cells was also seen after inhibition of caspase-3. Treatment of SK-N-BE(2) cells, transfected with PKC $\delta$ CD- or PKC $\theta$ RD-encoding vectors, with 50  $\mu$ M of the caspase-3 inhibitor Z-DEVD.fmk reduced the amount of apoptotic cells from 11.3 and 9.8 to 4.5 and 5.0%, respectively (Figure 3d). In TPA-treated SK-N-BE(2) cells overexpressing full-length PKC $\delta$  or PKC $\theta$ , Z-DEVD.fmk suppressed apoptosis from 12.2 or 13.0 to 5.2 and 6.8%, respectively (Figure 3e). Bcl-2

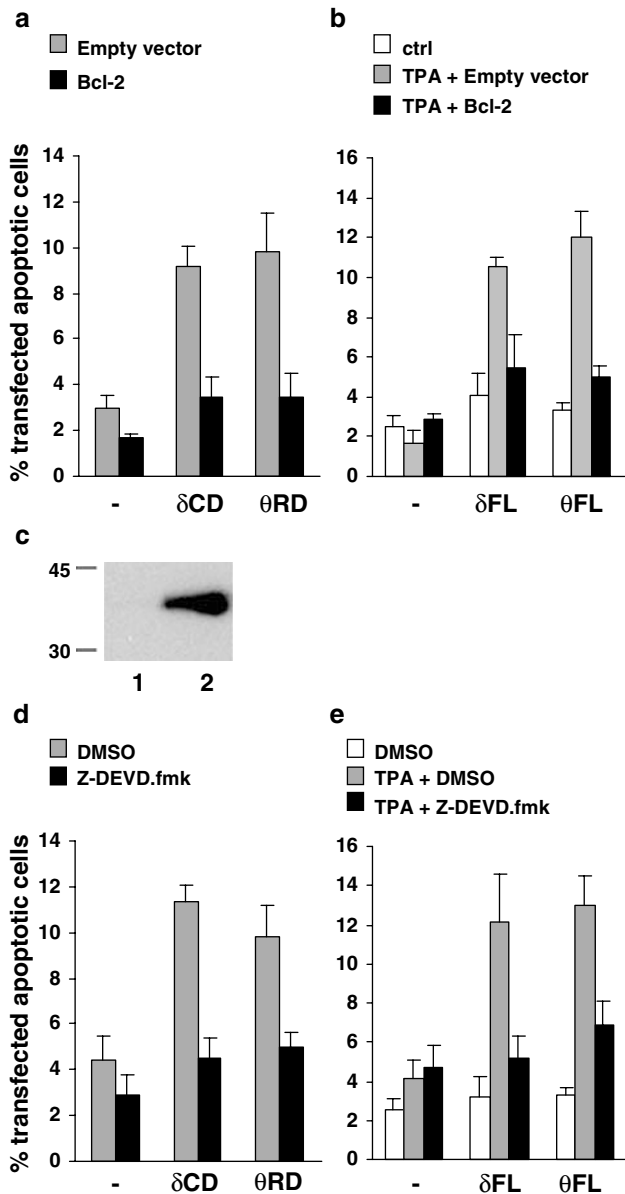


**Figure 3** Inhibition of the apoptotic effects of PKC $\delta$  and PKC $\theta$  constructs by Bcl-2 overexpression and caspase inhibition. (a) SK-N-BE(2) neuroblastoma cells were co-transfected with vectors encoding EGFP (–), PKC $\delta$ CD ( $\delta$ CD) or PKC $\theta$ RD ( $\theta$ RD) and an expression vector encoding Bcl-2 or an empty expression vector in a ratio 1:3. (b) SK-N-BE(2) cells were cotransfected with vectors encoding EGFP (–), PKC $\delta$ FL ( $\delta$ FL) or PKC $\theta$ FL ( $\theta$ FL) and an expression vector encoding Bcl-2 or an empty expression vector in a ratio 1:3. After transfection, cells were treated with 16 nM TPA or vehicle. (c) SK-N-BE(2) cells were transfected with the expression vector encoding Bcl-2 or an empty expression vector. An immunoblot was performed using an antibody specific for Bcl-2. The positions of the weight markers 45 and 30 kDa are shown to the left of the blot. (d) SK-N-BE(2) cells were transfected with expression vectors encoding EGFP (–), PKC $\delta$ CD ( $\delta$ CD) or PKC $\theta$ RD ( $\theta$ RD) fused to EGFP. (e) SK-N-BE(2) neuroblastoma cells were transfected with expression vectors encoding EGFP (–), PKC $\delta$ FL ( $\delta$ FL) or PKC $\theta$ FL ( $\theta$ FL) fused to EGFP. After transfection, cells in (d and e) were treated with 50  $\mu$ M Z-DEVD.fmk, an inhibitor of caspase-3, or vehicle (DMSO) and cells in (e) with either 16 nM TPA or vehicle. Cells in (a, b, d and e) were fixed 16 h after transfection and stained with propidium iodide. Transfected cells, visualised by the fluorescence of EGFP, were scored for apoptosis based on nuclear morphology. Data in (a, b, d and e) are expressed as percent transfected apoptotic cells (mean  $\pm$  S.E.M.,  $n=6$  (a and d),  $n=3$  (b and e))

and Z-DEVD.fmk did not have a major effect in cells expressing EGFP alone (Figure 3a, b, d and e).

### Both C1 and C2 domains are required for PKC $\theta$ RD-mediated apoptosis

Since the apoptotic effect of PKC $\delta$ CD is well characterised in other cell systems, we focused on the novel finding that the RD of PKC $\theta$  can induce apoptosis. To identify which parts of PKC $\theta$ RD that are essential for induction of apoptosis, four constructs encoding different parts of the domain were created (Figure 4a). All cDNAs were inserted into an expression vector containing EGFP cDNA. The vectors were transfected into SK-N-BE(2) cells and subjected to a Western blot analysis using an EGFP antibody to confirm that proteins of expected sizes were generated (Figure 4b). Transfection of SK-N-BE(2) cells with these constructs and scoring of transfected cells for apoptosis showed that 9.7% of PKC $\theta$ RD-expressing cells were apoptotic compared to 1.8% of cells expressing EGFP only (Figure 4c). Expression of the other constructs only caused a minor increase in apoptosis compared to expression of EGFP alone, an effect that was slightly enhanced after treatment of the transfected cells with 16 nM of TPA. Since Figure 4b indicates that the amount of expressed fusion proteins generated by the PKC $\theta$  constructs differed, the levels of EGFP fluorescence in single cells was analysed by laser scanning cytometry (Figure 4d). This experiment demonstrated that EGFP alone and PKC $\theta$ C2, PKC $\theta$ C2PS and PKC $\theta$ C2PSC1a were expressed at similar levels, whereas PKC $\theta$ RD and PKC $\theta$ PSC1V3 were expressed at lower levels. Thus, despite its low expression levels PKC $\theta$ RD is the most apoptotic construct. This suggests that both the C1 and the C2 domains are necessary for the apoptosis induction by PKC $\theta$ RD.

### TPA treatment does not induce cleavage of PKC $\delta$ or PKC $\theta$

Since the CDs of PKC $\delta$  and PKC $\theta$ , and the RD of PKC $\theta$  induced apoptosis when expressed in SK-N-BE(2) cells, we speculated that the apoptotic effect of TPA on SK-N-BE(2) cells overexpressing PKC $\delta$  and PKC $\theta$  was because of the cleavage of the PKC molecules into free RDs and CDs. To test this hypothesis, cells were transfected with expression vectors encoding full-length PKC $\delta$  or PKC $\theta$  fused to EGFP, treated with indicated combinations of TPA and GF109203X, and total cell lysates were analysed by Western blot using antibodies towards the CD of PKC $\delta$  and the RD of PKC $\theta$ , respectively. Protein bands of approximately 100 kDa corresponding to overexpressed full-length PKC $\delta$  (Figure 5a) and PKC $\theta$  (Figure 5b) fused to EGFP were detected in all cases. Cleavage of the PKC–EGFP proteins would have generated fragments of approximately 60 kDa (CD of PKC $\delta$  fused to EGFP) or 30 kDa (free RD of PKC $\theta$ ). We could not detect such fragments in neither immunoblot, which implies that the apoptotic response of TPA and GF109203X treatment is not because of proteolytic cleavage of the PKC isoforms.

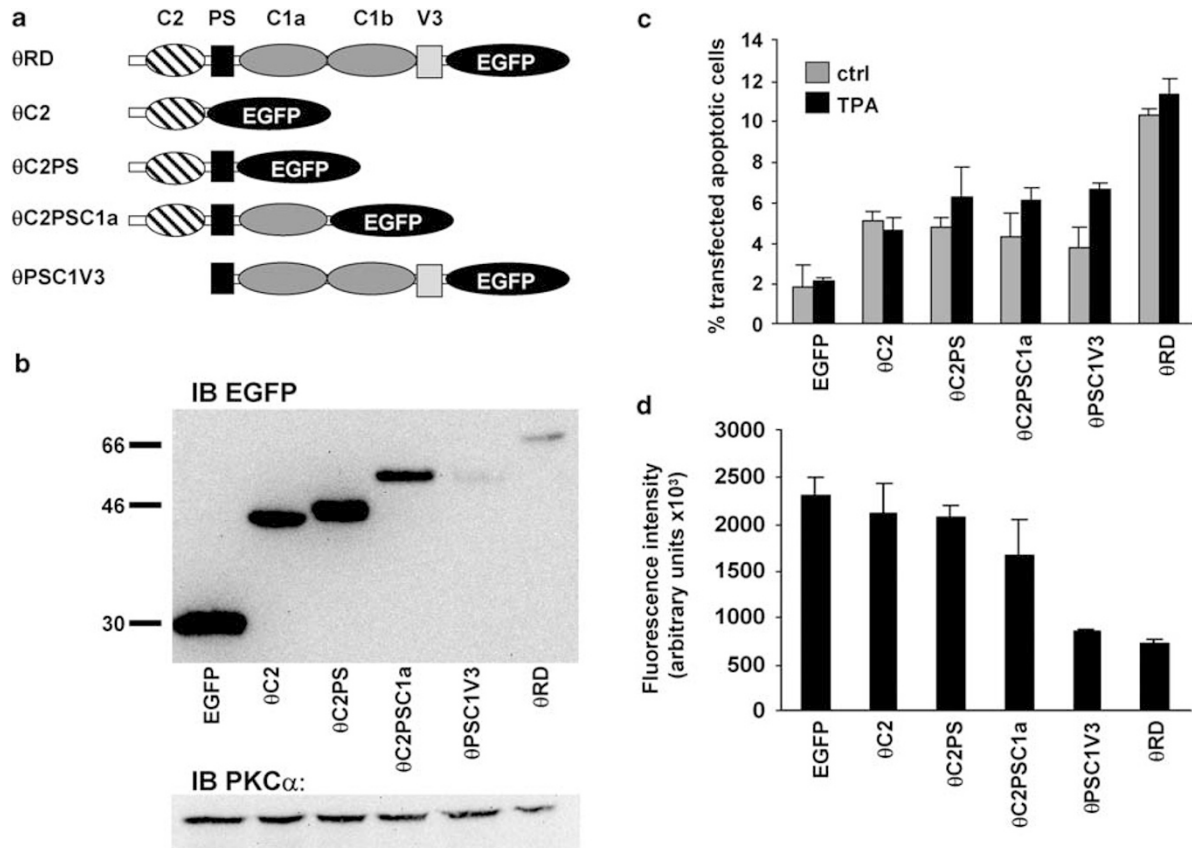


**Figure 4** Both C1 and C2 domains are required for apoptosis mediated by PKC $\theta$ RD. (a) Schematic presentation of the PKC $\theta$ -EGFP constructs used in this figure. The picture shows the pseudosubstrate (PS), C1, C2 and V3 domains. (b) SK-N-BE(2) cells were transfected with the EGFP-tagged PKC $\theta$  constructs described in (a) and the formation of protein products was analysed by Western blotting using an antibody towards EGFP (upper panel) or endogenous PKC $\alpha$  as a loading control (lower panel). The positions of the weight markers 66, 45 and 30 kDa are shown to the left of the blot. (c) SK-N-BE(2) cells were transfected with vectors encoding  $\theta$ RD,  $\theta$ C2,  $\theta$ C2PS or  $\theta$ C2PSC1a, all fused to EGFP or EGFP alone. After transfection, cells were treated with 16 nM TPA or vehicle. Cells were fixed and stained with propidium iodide 16 h after transfection. Transfected cells, visualised by the fluorescence of EGFP, were scored for apoptosis. Data (mean  $\pm$  SEM,  $n=3$ ) are presented as percent transfected apoptotic cells. (d) Expression levels in single cells of the EGFP fusion proteins were quantified with laser scanning cytometry. Data (mean  $\pm$  SEM,  $n=3$ , 150–200 cells analysed in each experiment) are arbitrary units of fluorescence intensity

### Expression of PKC $\theta$ RD induces cell death in Jurkat cells

We could not detect a cleavage of PKC $\delta$  or PKC $\theta$  in SK-N-BE(2) cells overexpressing these isoforms and induced to undergo apoptosis by TPA. However, the cleavage of these isoforms during the initiation of apoptosis has been described in several cells,<sup>4,7,8,11–14</sup> including T-cell lymphoma Jurkat cells during Fas-induced apoptosis.<sup>4</sup> We therefore examined the effect of expression of PKC $\delta$ CD and PKC $\theta$ RD in these cells. Jurkat cells were transfected by electroporation with expression vectors encoding PKC $\delta$ CD, PKC $\theta$ RD, PKC $\theta$ C2 and PKC $\theta$ PSC1V3, all fused to EGFP, or an empty EGFP vector. At 24 h after transfection, the cells were stained with biotinylated Annexin V and streptavidin-phycoerythrin and analysed for cell death by flow cytometry (Figure 6a). Of the Jurkat cells expressing PKC $\theta$ RD, 25% were Annexin V positive and consequently nonviable, whereas the corresponding number for cells expressing the other PKC $\theta$  constructs were lower; 14% for PKC $\theta$ C2 and 17% for PKC $\theta$ PSC1V3. This should be compared to 9% cell death upon transfection with empty EGFP vectors. Expression of PKC $\delta$ CD, which previously has been shown to induce

apoptosis in Jurkat cells, resulted in 45% cell death (Figure 6a). The expression levels of the different EGFP fusion proteins were also analysed (Figure 6b). As was the case in SK-N-BE(2) cells, PKC $\theta$ RD-EGFP was expressed at markedly lower levels than PKC $\theta$ C2. Thus, these experiments demonstrate that PKC $\theta$ RD also induces cell death in a cell in which the fragment is generated during the initiation of apoptosis, and that the effect of PKC $\theta$ RD is dependent on both the C1 and the C2 domains.

### Subcellular distribution of PKC $\theta$ constructs in SK-N-BE(2) and Jurkat cells

When analysing SK-N-BE(2) cells expressing different PKC $\theta$  domains fused to EGFP, we observed that the various PKC $\theta$  constructs displayed differences in their intracellular localisation (Figure 7A). EGFP, PKC $\theta$ C2, PKC $\theta$ C2PS and PKC $\theta$ C2PSC1a all localised throughout the cell, whereas fusion proteins containing both C1 domains, that is, PKC $\theta$ PSC1V3 and PKC $\theta$ RD, showed a prominent localisation to distinct punctuate structures that seemed to be enriched in the perinuclear area. A punctuate pattern of

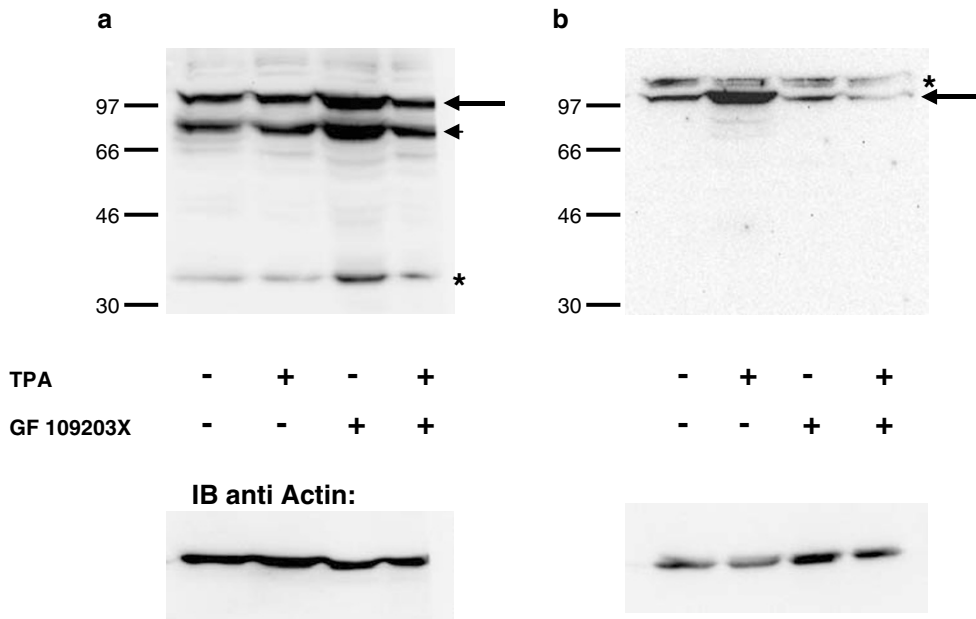


**Figure 5** TPA treatment does not induce cleavage of PKC $\delta$  or PKC $\theta$ . SK-N-BE(2) cells were transfected with expression vectors encoding full-length PKC $\delta$  (a) or PKC $\theta$  (b) fused to EGFP and treated with the indicated combinations of 16 nM TPA and/or 2  $\mu$ M GF109203X for 16 h. Total cell lysates were subjected to immunoblotting with antibodies towards the CD of PKC $\delta$  (a) and the RD of PKC $\theta$  (b). The positions of the weight markers 97, 66, 46 and 30 kDa are shown to the left of the blots. Arrows indicate reactivity corresponding to PKC-EGFP fusion proteins and the arrowhead demonstrates endogenous PKC $\delta$ . The stars denote unspecific bands, which also appeared in lysates from untransfected cells (not shown). The blots were stripped and reprobed for actin as a loading control (bottom panel). The results shown are representative of three independent experiments

PKC $\theta$ RD localisation was also observed in Jurkat cells (Figure 7B). Thus, when PKC $\theta$ RD is expressed in neuroblastoma or Jurkat cells it localises in a punctuate pattern and causes apoptosis. To elucidate whether endogenous PKC $\theta$  or PKC $\theta$ RD also localises in a similar pattern upon induction of apoptosis, we treated Jurkat cells with anti-Fas antibody, which has been shown to induce cleavage of PKC $\theta$  and release of the free RD.<sup>4</sup> This was followed by immunofluorescence with an antibody directed towards the PKC $\theta$ RD. With this approach both intact PKC $\theta$  and the free RD, but not the free CD, will be detected (Figure 7C). In untreated cells, PKC $\theta$  localised throughout the cytoplasm (Figure 7Ca), whereas upon anti-Fas treatment, a punctuate pattern of antibody staining was detected in a large proportion of the cells (Figure 7Cb and Cc). This indicates that after anti-Fas treatment, there is either a redistribution of full-length PKC $\theta$  to punctuate structures or a localisation to these structures by the released RD. This resembles the localisation of over-expressed PKC $\theta$ RD-EGFP, but whether the localisation pattern really is identical in the two cases remains to be proven.

### PKC $\theta$ RD localises to the Golgi complex

Since PKC $\theta$ RD displayed a similar punctuate localisation pattern in both SK-N-BE(2) and Jurkat cells at the same time as it induced apoptosis in these cells, we hypothesised that this localisation to specific intracellular structures may be of importance for the induction of apoptosis by PKC $\theta$ RD. To identify the intracellular compartment to which the PKC $\theta$ RD-EGFP fusion protein localises, SK-N-BE(2) cells were

transfected with the vector encoding this protein and subjected to staining with a series of markers for different organelles (Figure 8a) that have been suggested to be of importance in the regulation of apoptosis.<sup>25</sup> Colocalisation analysis revealed that PKC $\theta$ RD-EGFP neither localised to mitochondria (stained with Mitotracker Red), lysosomes (stained with LysoTracker Red) nor to early endosomes (visualised by immunofluorescence towards the marker EEA1).<sup>26</sup> However, a clear colocalisation with syntaxin 6, a marker for the *trans*-Golgi network<sup>27</sup> and with a marker for the *cis*-Golgi network, 58K,<sup>28</sup> was observed. Essentially all syntaxin 6- and 58K-positive structures were positive for PKC $\theta$ RD-EGFP, but PKC $\theta$ RD-EGFP also localised to punctuate structures that were negative for the markers. These results indicate that PKC $\theta$ RD to a large extent localises to the Golgi apparatus.

To further establish this finding, we treated PKC $\theta$ RD-EGFP-expressing cells with brefeldin A, which prevents trafficking from the endoplasmic reticulum to the Golgi and causes the Golgi complex to disassemble.<sup>29</sup> SK-N-BE(2) cells were exposed to 5  $\mu$ M brefeldin A for 1 h prior to staining with 58K and syntaxin 6 antibodies (Figure 8b). This treatment resulted in a loss of perinuclear staining of both Golgi markers (compare with Figure 8a), which now seemed to localise fairly uniformly throughout the cytoplasm, confirming the disassembly of the Golgi network. The perinuclear enrichment of PKC $\theta$ RD-EGFP was attenuated in brefeldin A-treated cells, but some PKC $\theta$ RD-positive punctuate structures could still be discerned. To follow the localisation of PKC $\theta$ RD-EGFP in the same cell during brefeldin A exposure, we followed live SK-N-BE(2) cells expressing the fusion protein during treatment with

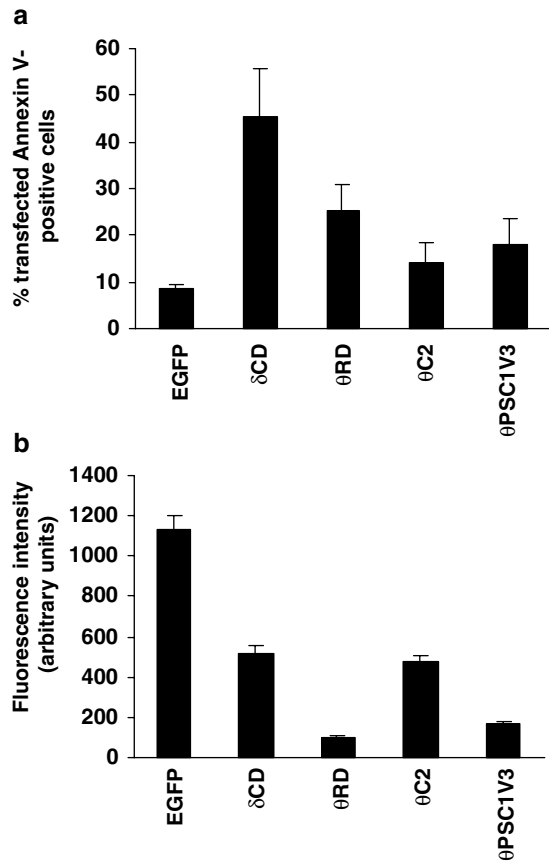


**Figure 6** Expression of PKC $\theta$ RD induces cell death in Jurkat cells. (a) Jurkat cells were transfected by electroporation with expression vectors encoding PKC $\Delta$ CD, PKC $\theta$ RD, PKC $\theta$ PSC1V3 or PKC $\theta$ C2 fused to EGFP or a vector encoding EGFP alone. 24 h after transfection, cells were stained with biotinylated Annexin V and streptavidin–phycoerythrin and analysed for cell death by flow cytometry. Data (mean  $\pm$  S.E.M.,  $n=5$ ) are presented as percent EGFP-positive cells that were Annexin V -positive. (b) Expression levels of the EGFP fusion proteins in single cells were quantified. Data (mean  $\pm$  SEM,  $n=5$ ) represent the mean fluorescence intensity in the FL1 channel and are presented as percent of the intensity of cells expressing EGFP alone

5  $\mu$ M brefeldin A (Figure 8c). Prior to brefeldin A addition there was a clear localisation of PKC $\theta$ RD–EGFP to perinuclear structures, but after 60 and 75 min of brefeldin A exposure this enrichment had diminished and there seemed to be an increase in the cytosol. There were also some punctuate PKC $\theta$ RD–EGFP-positive structures left in different areas of the cell. We therefore conclude that PKC $\theta$ RD localises to the Golgi apparatus, but also to other, so far unidentified, punctuate structures outside the Golgi apparatus.

### The C1b domain is necessary for localisation to the Golgi complex

The results presented in Figures 7 and 8 indicate that the C1 domains are required for a proper localisation of PKC $\theta$ RD to the Golgi complex. There are two C1 domains in PKC $\theta$ , C1a and C1b, and to investigate the relative importance of these domains for the localisation to the Golgi complex, three PKC $\theta$

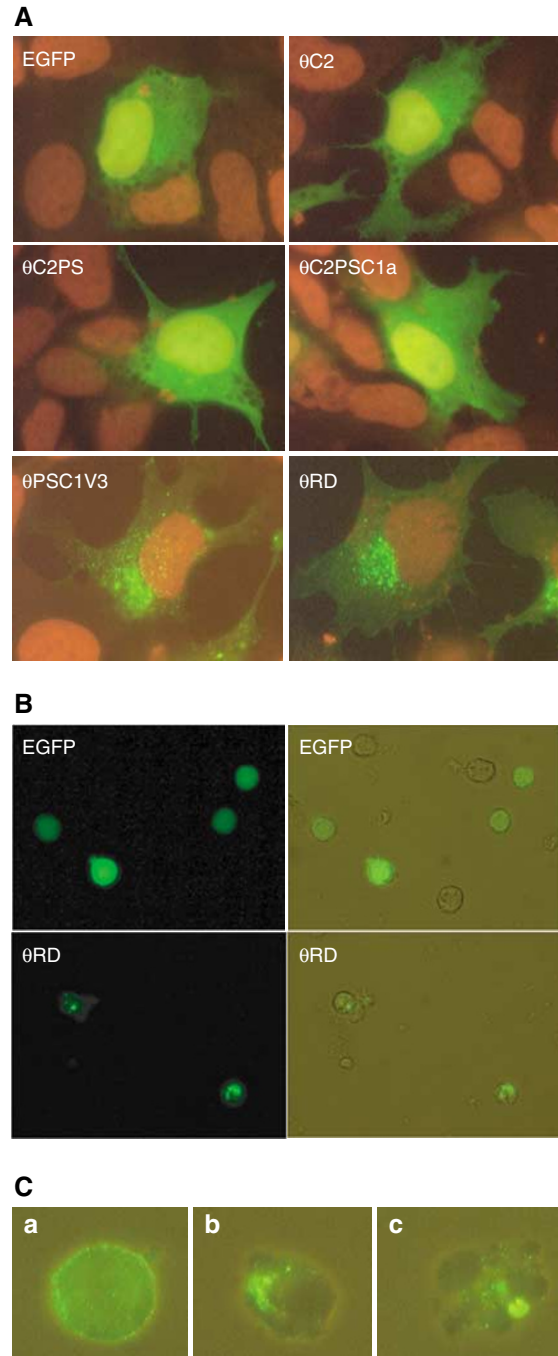


**Figure 7** Subcellular distribution of PKC $\theta$  constructs in SK-N-BE(2) and Jurkat cells. (A) SK-N-BE(2) cells were transfected with vectors encoding, PKC $\theta$ C2, PKC $\theta$ C2PS, PKC $\theta$ C2PSC1a, PKC $\theta$ PSC1V3 or PKC $\theta$ RD, all fused to EGFP or EGFP alone. Cells were fixed 16 h after transfection and nuclei were stained with propidium iodide. The localisation of the fusion proteins (green) and nuclei (red) was examined by fluorescence microscopy. (B) Jurkat cells were transfected by electroporation with expression vectors encoding PKC $\theta$ RD–EGFP or EGFP alone. 16 h after transfection, the cells were examined with a fluorescence microscope. For Jurkat cells, light microscopic images of the same fields are included to illustrate localisation of EGFP proteins in the cell. (c) Jurkat cells were incubated with 100 ng/ml anti-Fas antibody for 6 h. Cells were fixed and stained with antibodies towards PKC $\theta$ RD and Alexa Fluor 488-conjugated secondary antibodies and thereafter analysed by fluorescence microscopy. The images show untreated cells (Ca) and two different cells that were exposed to anti-Fas antibody (Cb and Cc)

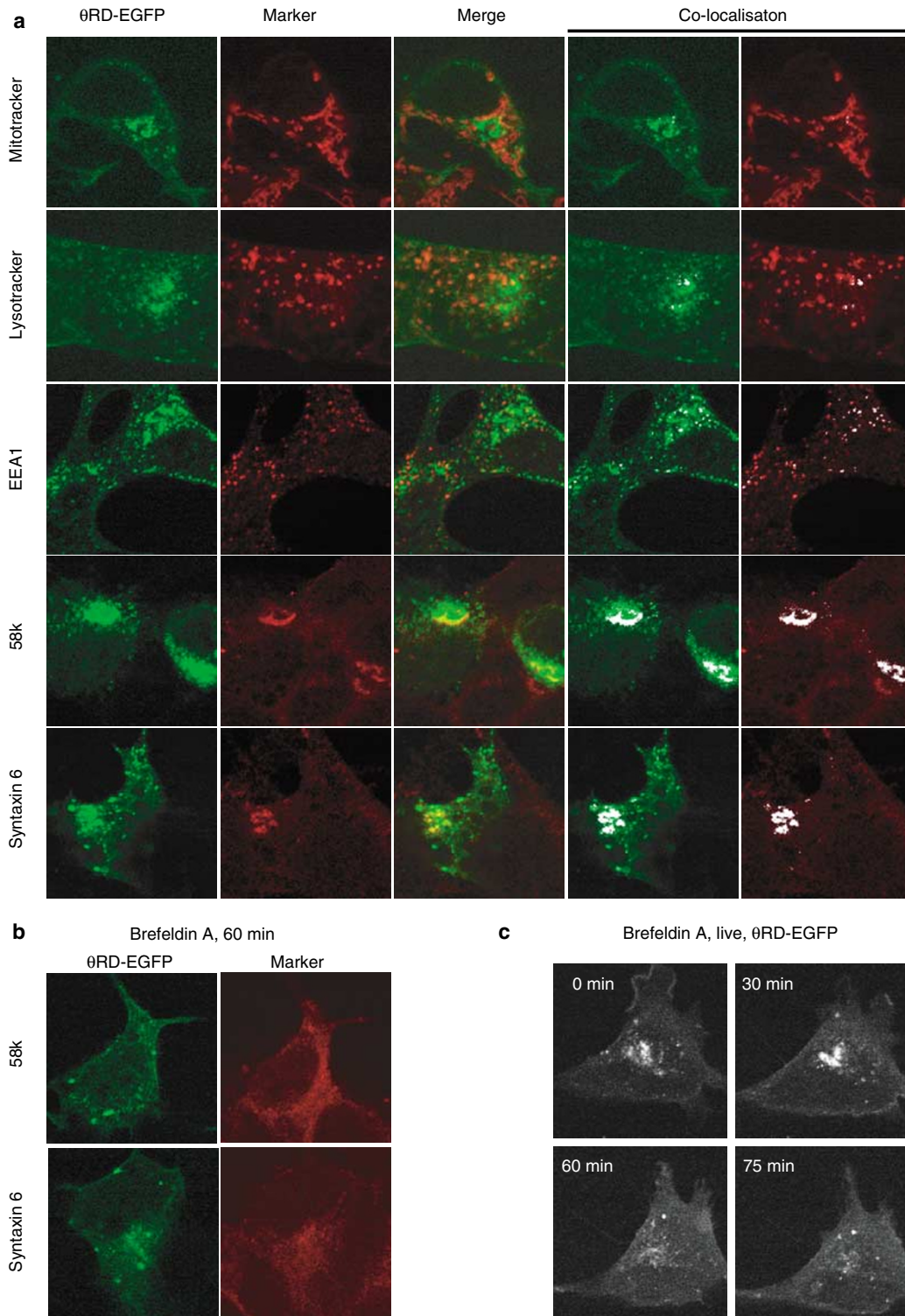


**Figure 8** PKC $\theta$ RD localises to the Golgi complex. SK-N-BE(2) cells were transfected with expression vectors encoding PKC $\theta$ RD fused to EGFP. (a) Different organelles in PKC $\theta$ RD-expressing cells were visualised. For visualisation of mitochondria and lysosomes, live cells were incubated with Mitotracker Red or Lysotracker Red and thereafter analysed by live confocal microscopy. For other organelles, transfected and fixed cells were stained with antibodies towards the early endosomal marker EEA1, the *cis*-Golgi marker 58 K or the *trans*-Golgi marker syntaxin 6 using Alexa Fluor 546-conjugated secondary antibodies and the cells were thereafter analysed by confocal microscopy. Colocalisation was analysed with the LaserPix software and pixels positive for both PKC $\theta$ RD and the structure markers are shown in white. (b) 16 h after transfection, PKC $\theta$ RD-EGFP-expressing cells were incubated with 5  $\mu$ M brefeldin A for 60 min. Cells were fixed and stained with antibodies towards the *cis*-Golgi marker 58 K or the *trans*-Golgi marker syntaxin 6 using Alexa Fluor 546-conjugated secondary antibodies and thereafter analysed by confocal microscopy. (c) 16 h after transfection, PKC $\theta$ RD-EGFP-expressing cells were treated with 5  $\mu$ M brefeldin A and the localisation of PKC $\theta$ RD-EGFP was followed by confocal microscopy for 75 min.



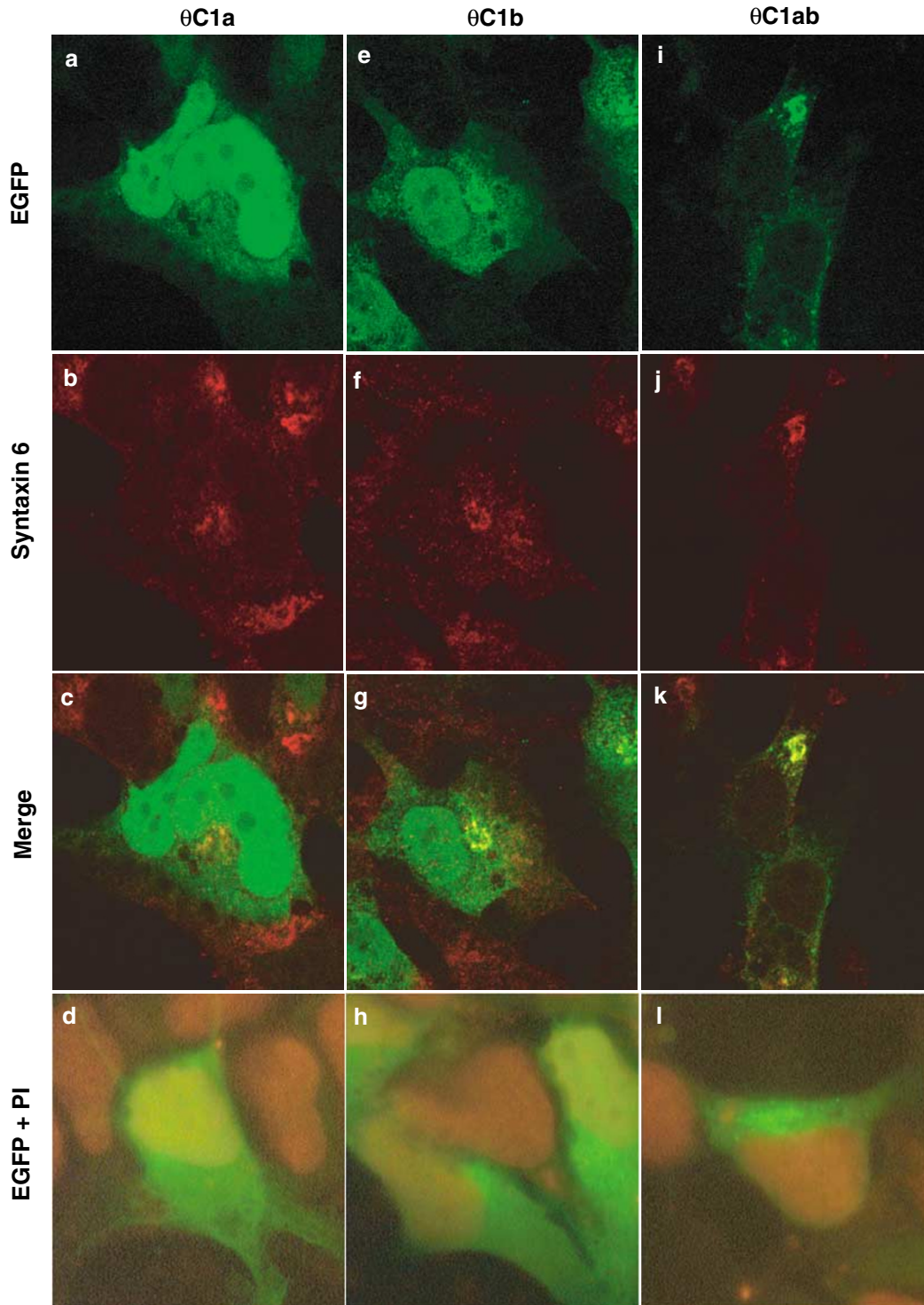


**Figure 9** The PKC $\theta$ C1b domain is necessary for localisation to the Golgi complex. SK-N-BE(2) cells were transfected with expression vectors encoding PKC $\theta$ C1a (a–d), PKC $\theta$ C1b (e–h) or PKC $\theta$ C1ab (i–l) fused to EGFP. Localisation of EGFP fusion proteins is shown in (a, e and i). At 16 h after transfection, cells were fixed and stained with the *trans*-Golgi marker syntaxin 6 using Alexa Fluor 546-conjugated secondary antibodies (b, f and j). Co-localisation was analysed by confocal microscopy and the merge of the PKC $\theta$  constructs and syntaxin 6 is shown in (c, g and k). For one set of cells (d, h and l), the nuclei were stained with propidium iodide and cells were examined with fluorescence microscopy

constructs encoding the isolated C1a domain (PKC $\theta$ C1a–EGFP), the isolated C1b domain (PKC $\theta$ C1b–EGFP) or both C1 domains (PKC $\theta$ C1ab–EGFP), all fused to EGFP, were

created. SK-N-BE(2) neuroblastoma cells were transfected with these plasmids, fixed and the *trans*-Golgi network was stained with antibodies towards syntaxin 6 and an Alexa Fluor

546-conjugated secondary antibody. Examination of the cells with confocal microscopy revealed that the PKC $\theta$ C1a-EGFP fusion protein localised throughout the cell (Figure 9a-d). Although PKC $\theta$ C1b-EGFP also had a tendency to be distributed throughout the cell, a major fraction colocalised with the marker of the *trans*-Golgi network (Figure 9e-h). Such a co-localisation was even more pronounced for PKC $\theta$ C1ab-EGFP, which displayed a distinct localisation to the Golgi complex (Figure 9i-l). In conclusion, these data suggest that the C1b domain of PKC $\theta$  is the most important structure for localisation of PKC $\theta$  to the Golgi complex.

## Discussion

This study demonstrates apoptotic effects of PKC $\delta$  and PKC $\theta$  in neuroblastoma cells. An abundance of studies has previously implicated PKC $\delta$  in the onset of apoptosis, but also PKC $\theta$  has been suggested to have proapoptotic effects. Both PKC $\delta$ <sup>4,7,8,11-13</sup> and PKC $\theta$ <sup>4,14</sup> are cleaved by caspases generating free CDs and RDs and overexpression of the CD of PKC $\delta$ <sup>4,12,15</sup> or PKC $\theta$ <sup>14</sup> induces apoptosis in a wide range of cells. This study demonstrates that this is also the case in neuronal cells further underscoring the generality of the apoptotic effect of the PKC $\delta$  and PKC $\theta$  CDs. The effect was suppressed by the PKC inhibitor GF109203X, demonstrating the dependence on the catalytic activity of the kinase.

However, PKC $\delta$ -mediated apoptosis without proteolytic cleavage of the enzyme has also been reported.<sup>30</sup> That is analogous to what we observed after TPA treatment of neuroblastoma cells overexpressing PKC $\delta$  or PKC $\theta$ , in which we could not detect a proteolytic cleavage of PKC $\delta$  or PKC $\theta$ . In addition, it has been suggested that either mitochondrial<sup>9,10,31</sup> or nuclear<sup>32-34</sup> translocation is essential for PKC $\delta$  to induce apoptosis and the former has been associated with the trigger of a ceramide-PKC $\delta$  amplification loop.<sup>9</sup> Thus, there may be different mechanisms through which PKC $\delta$  induces apoptosis. In our study, GF109203X suppressed the apoptotic effect of the free catalytic fragments of PKC $\delta$  and PKC $\theta$ , but had no attenuating effect on cell death induced by TPA treatment of cells overexpressing full-length PKC $\delta$  or PKC $\theta$ . Thus, although the free, constitutively active catalytic fragment of PKC $\delta$  or PKC $\theta$  induces apoptosis in neuroblastoma cells, induction of cell death by full-length PKC $\delta$  or PKC $\theta$  neither involves the cleavage of the kinases nor the activity of them. This suggests that the free CD and the full-length proteins exert their apoptotic effects via different mechanisms in neuroblastoma cells.

The result that PKC $\delta$  and PKC $\theta$  induction of apoptosis is independent of the kinase activity of the enzymes is in line with the recently published finding in aortic smooth muscle cells.<sup>35</sup> Our study therefore indicates that such an effect of PKC $\delta$  may be general and not limited to one specific cell type. It further emphasises that there may be several different pathways coupling PKC $\delta$  to induction of apoptosis.

Similar to what was observed in aortic smooth muscle cells,<sup>35</sup> we found that TPA only induced apoptosis in cells overexpressing PKC $\delta$  or PKC $\theta$  despite the fact that neuroblastoma cells express both these isoforms.<sup>36,37</sup> This could be because of the fact that TPA treatment simultaneously will

activate all classical and novel PKC isoforms and other phorbol ester-sensitive proteins such as chimaerins and the ras exchange factor RAS-GRF,<sup>38</sup> which possibly could counteract the apoptotic action of endogenous PKC $\delta$  and PKC $\theta$ . Such a counteractive effect could for instance be mediated by classical PKC isoforms since we have seen that an inhibitor of these isoforms induces apoptosis in neuroblastoma cells.<sup>37</sup> Selective activation of endogenous PKC $\delta$  or PKC $\theta$  may therefore be an interesting strategy to force neuroblastoma cells into apoptosis.

Our data also demonstrate that the RD of PKC $\theta$  by itself elicits apoptosis. There are now accumulating evidences that PKC can mediate some of its molecular and biological effects via the RD, independently of its kinase activity.<sup>39-42</sup> However, RDs of PKC isoforms have also been suggested to act as isoform-specific dominant-negative inhibitors.<sup>43</sup> Since PKC $\theta$  has been reported to exert antiapoptotic activity,<sup>16,18</sup> a dominant-negative effect towards PKC $\theta$  could possibly explain the apoptotic effect of PKC $\theta$ RD. In line with this reasoning, it could be argued that the apoptotic effect of TPA on cells overexpressing PKC $\delta$  or PKC $\theta$  is because of a downregulation of the isoforms and thus a consequence of an inactivation of the kinases. However, several of our findings speak against these alternatives. The levels of PKC $\delta$ -EGFP and PKC $\theta$ -EGFP were not downregulated by TPA treatment. The TPA effect may therefore conceivably be because of its direct interaction with the overexpressed isoform and may be related to a change in conformation or localisation of the protein. Furthermore, the fact that TPA leads to apoptosis only in cells overexpressing PKC $\delta$  or PKC $\theta$  is difficult to fit into a model where the apoptotic effect of PKC $\theta$ RD is caused by it being dominant negative. If the induction of apoptosis by PKC $\theta$ RD is a dominant-negative effect, it would be expected that TPA stimulation of cells overexpressing PKC $\theta$  would not be proapoptotic, as it is. It is possible that the RD of PKC $\theta$  actually mimics the effect of TPA-treated full-length PKC $\theta$  in the induction of apoptosis in neuroblastoma cells or that the free RD exerts effects that are unrelated to the action of full-length PKC $\theta$  and therefore mediated through another pathway when leading to apoptosis.

However, there is at least one common denominator for the apoptotic pathways induced by the full-length PKC $\delta$  and PKC $\theta$ , the CD of PKC $\delta$  and PKC $\theta$  and of PKC $\theta$ RD. In all cases, the induction apoptosis was suppressed by both Bcl-2 overexpression and by inhibition of caspase-3. This suggests that there is an involvement of the mitochondrial apoptotic pathway, which includes the release of cytochrome *c* with subsequent activation of caspases-3 and 8, (reviewed in Hengartner<sup>24</sup>). However, it should be noted that Bcl-2 localises to other organelles as well<sup>44-46</sup> and caspase-3 is a common target for several apoptotic inducers. It can therefore not be excluded that other organelles than mitochondria are the main targets in the apoptotic induction by the different PKC constructs.

In this context, we found the specific subcellular distribution pattern of PKC $\theta$ RD both in neuroblastoma and Jurkat cells interesting. By costaining for markers of different organelles, we could conclude that PKC $\theta$ RD to a large extent localises to the Golgi complex in neuroblastoma cells. However, there were also distinct punctuate PKC $\theta$ RD-positive structures,

which we so far have been unable to identify. The localisation was mediated by and dependent on the second C1 (C1b) domain of PKC $\theta$ . There are several reports showing that C1 domain-containing proteins are targeted to the Golgi complex.<sup>39,47–49</sup> However, not all C1 domains, as exemplified by PKC $\theta$  C1a in this study, have this localisation pattern. So far, Golgi localisation has been observed for several isolated C1 domains including the C1 domain of chimaerins,<sup>47</sup> the C1b domain of PKC $\epsilon$ <sup>48</sup> and the C1a domain of PKD.<sup>49</sup> It will be of interest to determine whether these C1 domains have structures in common that determine their localisation pattern. It is conceivable that targeting to the Golgi network may be because of interaction with Golgi proteins and one such candidate, Tmp21-1,<sup>50</sup> has been identified as an interaction partner of the  $\beta$ 2-chimaerin C1 domain. The C1-mediated localisation has also been shown to be dependent on diacylglycerol production as demonstrated for the PKD C1a domain.<sup>51</sup>

When the C1b domain was deleted from PKC $\theta$ RD, generating PKC $\theta$ C2PSC1a, both localisation to the Golgi and induction of apoptosis was abrogated. We therefore speculate that targeting to the Golgi complex is of importance for the apoptotic effect of PKC $\theta$ RD. The Golgi apparatus has been shown to harbour several apoptosis-signalling proteins such as caspase-2,<sup>52</sup> Fas/CD95,<sup>53</sup> and GD3 synthase.<sup>54</sup> The Golgi membranes have also been suggested to be a site of ceramide signalling.<sup>55</sup> Taken together, these facts imply that the Golgi complex is a potentially important site for proapoptotic signal transduction.

The PKC $\theta$ RD construct with deleted C2 domain, PKC $\theta$ PSC1V3, seemed to have a similar distribution pattern as the intact PKC $\theta$ RD but had a smaller apoptotic effect. This suggests that the C2 domain also plays a role for the apoptotic response. The C2 domains of different PKC isoforms have been shown to be important for the interaction of PKC with several proteins, among others the RACKs, receptors for activated C-kinases.<sup>56</sup> A speculative model is that the role of the C1 domains may be to target PKC $\theta$ RD to the Golgi apparatus where the C2 domain could interact with other

target protein, an interaction that could be of importance for induction of apoptosis.

In conclusion, this study suggests that selective activation of the novel PKC isoforms PKC $\delta$  and PKC $\theta$  could be a successful approach to elicit apoptosis in neuroblastoma cells. We also demonstrate that the RD of PKC $\theta$  induces apoptosis, an effect that is correlated to a localisation to the Golgi complex.

## Materials and Methods

### Plasmids

Plasmids encoding the RDs of human PKC isoforms  $\alpha$ ,  $\beta$ ,  $\delta$ ,  $\epsilon$ ,  $\eta$  and  $\theta$  and full-length PKC  $\delta$ ,  $\epsilon$  and  $\theta$  fused to EGFP have been described.<sup>41</sup> cDNA encoding the C1a, C1b, C1ab, C2, C2PS, C2PSC1V3 and PSC1V3 regions of PKC $\theta$  and CDs of PKC $\delta$ ,  $\epsilon$  and  $\theta$  were generated by PCR using plasmids encoding the full-length PKC isoforms as template. The PCR reactions were performed with *Pfu* polymerase (Promega) to minimise introduction of mutations. Restriction enzyme sites were introduced in the primers (Table 1) enabling the ligation of the PCR product in the EGFP-N1 vector (Clontech). All PKC cDNAs were sequenced to ensure that no mutations were introduced in the PCR reactions. The Bcl-2 expression vector was kindly provided by Dr. Stanley Korsmeyer.<sup>57</sup>

### Cell culture and transfections

Human neuroblastoma SK-N-BE(2), SK-N-SH and KCN-69n cells were cultured in minimum essential medium supplemented with 10% fetal bovine serum, 100 IU/ml penicillin and 100  $\mu$ g/ml streptomycin. For transfection experiments, cells were trypsinised and seeded at a density of 300 000 cells per 35-mm cell culture dish on glass coverslips in medium containing serum and antibiotics. Transfections were initiated 24 h after seeding. Prior to transfection, cells were washed with serum-free medium. Cells were transfected using 5  $\mu$ l Lipofectamine 2000 (Invitrogen) and 1.6  $\mu$ g DNA according to the supplier's protocol. When indicated, TPA (Sigma), GF109203X (Calbiochem) and Z-DEVD.fmk (Calbiochem) were used at concentrations of 16 nM, 2  $\mu$ M and 50  $\mu$ M, respectively. Ethanol or DMSO was added to the control to get the same solvent concentration.

**Table 1** Primers used to generate new PKC constructs

Construct	Primers
PKC $\delta$ CD	Forward: CGCCTCGAGCCCACCATGGGTTTCGAGAAGAAGACCGGA Reverse: AATTCGAGCACCTCCTGGAAGATCGAATTCGCG
PKC $\epsilon$ CD	Forward: GCGAGATCTCGACCATGAGCCCCGGTGAGAATGGC Reverse: GGTGAAGACCTGATGCCCTGGTCGACGCG
PKC $\theta$ CD	Forward: GCGGGATCCCCATGTGCCATCTTCCAGAACCT Reverse: GGGATGGAGCGGCTGATATCGTCGACCGC
PKC $\theta$ C2	Forward: GCGGGATCCCAACCATGTCCGCAATTTCTTCGGA Reverse: GCGGTCGACTCCGTCTCAAATTCATTCATGTC
PKC $\theta$ C2PS	Forward: GCGGGATCCCAACCATGTCCGCAATTTCTTCGGA Reverse: GGCAAAGGTCCACCACGTCAAGTCGACGCG
PKC $\theta$ C2PSC1a	Forward: GCGGGATCCCAACCATGTCCGCAATTTCTTCGGA Reverse: ATCAATAGCCGAGAAACCATGTCCGACGCG
PKC $\theta$ PSC1V3	Forward: GCGGGATCCCAACCATGGACACAAAGGACATGAATGAATT Reverse: GAGCCTCAGGGCATTTCCTGGTCGACAGC
PKC $\theta$ C1a	Forward: GCGAGATCTCGACCATGCACGTCAAGTGCCACGAGTTC Reverse: CAAGGAGAGATTCAAAATTGAGTCGACGCG
PKC $\theta$ C1b	Forward: GCGAGATCTCGACCATGATTGACATGCCACACAGATTT Reverse: ATTGAGAGCACTCAACAGGCGTCGACGCG
PKC $\theta$ C1ab	Forward: GCGAGATCTCGACCATGCACGTCAAGTGCCACGAGTTC Reverse: ATTGAGAGCACTCAACAGGCGTCGACGCG

Human T-cell lymphoma Jurkat cells were cultured in RPMI 1640 medium supplemented with 10% heat-inactivated fetal bovine serum, 25 mM HEPES, 50  $\mu$ M  $\beta$ -mercaptoethanol, 100 IU/ml penicillin and 100  $\mu$ g/ml streptomycin. Jurkat cells were suspended at a density of  $1 \times 10^7$  cells/ml and transfected by electroporation (Gene Pulsar, Bio-Rad; 0.4 cm cuvettes, 280 V, 950  $\mu$ F). At 3 h after transfection, dead cells were removed using a Ficoll (Amersham Biosciences) density gradient. In some experiments, Jurkat cells were treated with 100 ng/ml anti-Fas antibody CH11 (MBL) for 6 h.

### Analysis of apoptosis

At 16 h after transfection, neuroblastoma cells were fixed in 4% paraformaldehyde in PBS for 4 min and permeabilised with 0.1% Triton-X 100 and 0.1% sodium citrate in PBS for 2 min on ice. Cells were washed in PBS and then incubated with DNase-free RNase A (1 mg/ml in PBS) at 37°C for 45 min followed by staining of the nuclei with propidium iodide (5  $\mu$ g/ml in PBS) for 30 min at room temperature. Thereafter, cells were washed in PBS and mounted on microscopy slides using PVA-DABCO (9.6% polyvinylalcohol, 24% glycerol and 2.5% 1,4-diazabicyclo (2.2.2) octane in 67 mM Tris-HCl, pH 8.0). A total of 200 transfected cells, visualised by the fluorescence of EGFP, were counted per experiment and scored for apoptosis based on the morphology of the nucleus, which was visualised by propidium iodide. Cells were examined by fluorescence microscopy using standard FITC and TRITC filters.

### Laser scanning cytometry

The amount of PKC-EGFP fusion proteins in individual cells was estimated with a laser scanning cytometer (CompuCyte) using a  $\times 20$  objective applying 488 nm excitation and a 530/30 emission filter. The levels of laser strength and detection gain were set so that no pixel of PKC-EGFP-expressing cells reached saturation, and these settings were the same for all experiments. After the scan, each cell was relocated to ensure that only single cells were used for quantification.

### Immunofluorescence

SK-N-BE(2) cells were fixed with 4% paraformaldehyde in PBS for 4 min, permeabilised and blocked with 5% normal goat serum and 0.3% Triton X-100 in TBS for 30 min. Golgi 58 K protein, EEA1 and syntaxin 6 were detected with primary monoclonal mouse antibodies (Sigma, BD Transduction Laboratories and BD Transduction Laboratories, respectively) diluted 1 : 100, 1 : 25 and 1 : 25, respectively, in TBS followed by the secondary antibody Alexa Fluor 546-conjugated goat anti-mouse (Molecular Probes) diluted 1 : 400 in TBS. Both incubations were 1 h in length. Extensive washing was carried out between all steps and the cover-slips were mounted on object slides. Jurkat cells were fixed with 4% paraformaldehyde in PBS for 4 min and washed three times in PBS. Blocking and permeabilisation of the cells were performed in 5% normal goat serum and 0.3% Triton X-100 in PBS for 30 min. Jurkat cells were stained with primary monoclonal antibodies towards PKC $\theta$ RD (Transduction Laboratories) diluted 1 : 25 in TBS, followed by the secondary antibody Alexa Fluor 488-conjugated goat anti-mouse diluted 1 : 400 in TBS. Both incubations were 1 h in length. Extensive washing was carried out between all steps and the coverslips were mounted on object slides. Jurkat cells were examined by fluorescence microscopy using standard FITC and TRITC filters.

### Confocal microscopy

Live SK-N-BE(2) cells were examined by confocal microscopy on the day after transfection. Mitochondria and lysosomes were stained for 15 min at 37°C with 50 nM Mitotracker Red and 900 nM LysoTracker Red (Molecular Probes), respectively. The cover-slips were washed twice with buffer H (20 mM HEPES, 137 mM NaCl, 3.7 mM KCl, 1.2 mM MgSO<sub>4</sub>, 2.2 mM KH<sub>2</sub>PO<sub>4</sub>, 1.6 mM CaCl<sub>2</sub>, and 10 mM glucose; pH 7.4) and mounted on the heated stage of a Nikon microscope. To study the localisation of PKC $\theta$ RD-EGFP in the same cell after brefeldin A addition, 5  $\mu$ M brefeldin A (Calbiochem) was added to the buffer and the localisation of PKC $\theta$ RD-EGFP was followed for 75 min. The cells were examined using a 60 $\times$  objective (NA 1.4) and a Bio-Rad Radiance 2000 confocal system with excitation wavelengths at 488 nm (EGFP) and 543 nm (Mitotracker/LysoTracker Red) and emission filters 515HQ30 (EGFP) and 600LP (Mitotracker/LysoTracker Red). Alexa Fluor 546 immunofluorescence experiments on fixed cells were examined with excitation wavelengths at 543 nm and emission filters 600LP. Colocalisation was analysed with the LaserPix software.

### Western blot

SK-N-BE(2) cells were transfected, washed with PBS and lysed in RIPA buffer (10 mM Tris-HCl pH 7.2, 160 mM NaCl, 1% Triton-X 100, 1% sodium deoxycholate, 0.1% sodium dodecyl sulfate, 1 mM EDTA, 1 mM EGTA) containing 40  $\mu$ l/ml of protease inhibitor (Roche). Lysates were centrifuged for 10 min at 14,000  $\times$  g, 4°C, and protein concentrations were determined. Equal amounts of proteins were electrophoretically separated on an SDS-polyacrylamide gel and transferred to a Hybond-C nitrocellulose filter (Amersham Biosciences). Proteins were analysed with primary antibodies towards Bcl-2 (Santa Cruz Biotechnology) diluted 1 : 500, EGFP (Babco) diluted 1 : 1000, PKC $\alpha$  (Upstate Biotechnology) diluted 1 : 500, PKC $\delta$  (Santa Cruz Biotechnology) diluted 1 : 200, PKC $\theta$  (BD Transduction Laboratories) diluted 1 : 200 and actin (ICN Biomedicals) diluted 1 : 2000, and visualised with horse-radish peroxidase labelled secondary antibodies (Amersham Biosciences) using the SuperSignal system (Pierce Chemical) as substrate. The chemiluminescence was detected with a CCD camera (Fuji Film).

### Flow-cytometric analysis

Transfected Jurkat cells were stained with Annexin V-biotin (R&D Systems) and streptavidin-phycoerythrin (DAKO). Two-colour analysis was performed on a FACSCalibur cytometer (Becton Dickinson), where the EGFP signal was acquired on the FL-1 channel and the Annexin V signal on the FL-2 channel using log amplifications. Sample acquisition and analysis were performed with CellQuest software (Becton Dickinson). In all, 10 000 events were acquired from each sample using a broad forward and side scatter gate, so that only few cells were excluded from the data. Untransfected Jurkat cells were used as negative control in both channels, whereas etoposide-treated Jurkat cells were used as positive controls for Annexin V-staining.

### Acknowledgements

We thank Dr. Stanley Korsmeyer for providing the Bcl-2 expression vector. Financial support was obtained from The Swedish Cancer Society, The Children's Cancer Foundation of Sweden, The Swedish Society for Medical Research, Malmö University Hospital Research Funds, and

Magnus Bergvall, Crafoord, Ollie and Olof Ericsson and Gunnar Nilsson Foundation.

## References

- Newton AC (1995) Protein kinase C: structure, function, and regulation. *J. Biol. Chem.* 270: 28495–28498
- Nishizuka Y (1992) Intracellular signaling by hydrolysis of phospholipids and activation of protein kinase C. *Science*, 258: 607–614
- Stabel S and Parker PJ (1991) Protein kinase C. *Pharmacol. Ther.* 51: 71–95
- Mizuno K, Noda K, Araki T, Imaoka T, Kobayashi Y, Akita Y, Shimonaka M, Kishi S and Ohno S (1997) The proteolytic cleavage of protein kinase C isoforms, which generates kinase and regulatory fragments, correlates with Fas-mediated and 12-*O*-tetradecanoyl-phorbol-13-acetate-induced apoptosis. *Eur. J. Biochem.* 250: 7–18
- Majumder PK, Mishra NC, Sun X, Bharti A, Kharbanda S, Saxena S and Kufe D (2001) Targeting of protein kinase C  $\delta$  to mitochondria in the oxidative stress response. *Cell Growth. Differ.* 12: 465–470
- Shizukuda Y, Reyland ME and Buttrick PM (2002) Protein kinase C- $\delta$  modulates apoptosis induced by hyperglycemia in adult ventricular myocytes. *Am. J. Physiol. Heart. Circ. Physiol.* 282: H1625–H1634
- Denning MF, Wang Y, Nickoloff BJ and Wrone-Smith T (1998) Protein kinase C $\delta$  is activated by caspase-dependent proteolysis during ultraviolet radiation-induced apoptosis of human keratinocytes. *J. Biol. Chem.* 273: 29995–30002
- Reyland ME, Anderson SM, Matassa AA, Barzen KA and Quissell DO (1999) Protein kinase C $\delta$  is essential for etoposide-induced apoptosis in salivary gland acinar cells. *J. Biol. Chem.* 274: 19115–19123
- Sumitomo M, Ohba M, Asakuma J, Asano T, Kuroki T and Hayakawa M (2002) Protein kinase C $\delta$  amplifies ceramide formation via mitochondrial signaling in prostate cancer cells. *J. Clin. Invest.* 109: 827–836
- Li L, Lorenzo PS, Bogi K, Blumberg PM and Yuspa SH (1999) Protein kinase C $\delta$  targets mitochondria, alters mitochondrial membrane potential, and induces apoptosis in normal and neoplastic keratinocytes when overexpressed by an adenoviral vector. *Mol. Cell. Biol.* 19: 8547–8558
- Emoto Y, Kisaki H, Manome Y, Kharbanda S and Kufe D (1996) Activation of protein kinase C $\delta$  in human myeloid leukemia cells treated with 1- $\beta$ -D-arabinofuranosylcytosine. *Blood*. 87: 1990–1996
- Ghayur T, Hugunin M, Talanian RV, Ratnoffsky S, Quinlan C, Emoto Y *et al.* (1996) Proteolytic activation of protein kinase C  $\delta$  by an ICE/CED 3-like protease induces characteristics of apoptosis. *J. Exp. Med.* 184: 2399–2404
- Shao RG, Cao CX and Pommier Y (1997) Activation of PKC $\alpha$  downstream from caspases during apoptosis induced by 7-hydroxystaurosporine or the topoisomerase inhibitors, camptothecin and etoposide, in human myeloid leukemia HL60 cells. *J. Biol. Chem.* 272: 31321–31325
- Datta R, Kojima H, Yoshida K and Kufe D (1997) Caspase-3-mediated cleavage of protein kinase C  $\theta$  in induction of apoptosis. *J. Biol. Chem.* 272: 20317–20320
- Bharti A, Kraeft SK, Gounder M, Pandey P, Jin S and Yuan ZM *et al.* (1998) Inactivation of DNA-dependent protein kinase by protein kinase C $\delta$ : implications for apoptosis. *Mol. Cell. Biol.* 18: 6719–6728
- Bertolotto C, Maulon L, Filippa N, Baier G and Auberger P (2000) Protein Kinase C  $\theta$  and  $\varepsilon$  Promote T-cell Survival by a Rsk-dependent phosphorylation and inactivation of BAD. *J. Biol. Chem.* 275: 37246–37250
- Gubina E, Rinaudo MS, Szallasi Z, Blumberg PM and Mufson RA (1998) Overexpression of protein kinase C isoform  $\varepsilon$  but not  $\delta$  in human interleukin-3-dependent cells suppresses apoptosis and induces bcl-2 expression. *Blood*. 91: 823–829
- Villalba M, Bushway P and Altman A (2001) Protein kinase C- $\theta$  mediates a selective T cell survival signal via phosphorylation of BAD. *J. Immunol.* 166: 5955–5963
- Whelan RD, Parker PJ (1998) Loss of protein kinase C function induces an apoptotic response. *Oncogene*. 16: 1939–1944
- Ruvolo PP, Deng X, Carr BK and May WS (1998) A functional role for mitochondrial protein kinase C $\alpha$  in Bcl2 phosphorylation and suppression of apoptosis. *J. Biol. Chem.* 273: 25436–25442
- Gomez-Angelats M and Cidlowski JA (2001) Protein kinase C regulates FADD recruitment and death-inducing signaling complex formation in Fas/CD95-induced apoptosis. *J. Biol. Chem.* 276: 44944–44952
- Garcia-Bermejo ML, Leskow FC, Fujii T, Wang Q, Blumberg PM, Ohba M *et al.* (2002) Diacylglycerol (DAG)-lactones, a new class of protein kinase C (PKC) agonists, induce apoptosis in LNCaP prostate cancer cells by selective activation of PKC $\alpha$ . *J. Biol. Chem.* 277: 645–655
- Gschwend JE, Fair WR, Powell CT (2000) Bryostatin 1 induces prolonged activation of extracellular regulated protein kinases in and apoptosis of LNCaP human prostate cancer cells overexpressing protein kinase  $\alpha$ . *Mol. Pharmacol.* 57: 1224–1234
- Hengartner MO (2000) The biochemistry of apoptosis. *Nature* 407: 770–776
- Ferri KF and Kroemer G (2001) Organelle-specific initiation of cell death pathways. *Nat. Cell. Biol.* 3: E255–E263
- Mu FT, Callaghan JM, Steele-Mortimer O, Stenmark H, Parton RG, Campbell PL *et al.* (1995) EEA1, an early endosome-associated protein. EEA1 is a conserved alpha-helical peripheral membrane protein flanked by cysteine 'fingers' and contains a calmodulin-binding IQ motif. *J. Biol. Chem.* 270: 13503–13511
- Bock JB, Klumperman J, Davanger S and Scheller RH (1997) Syntaxin 6 functions in trans-Golgi network vesicle trafficking. *Mol. Biol. Cell.* 8: 1261–1271
- Kamishohara M, Kenney S, Domergue R, Vistica DT and Sausville EA (2000) Selective accumulation of the endoplasmic reticulum–Golgi intermediate compartment induced by the antitumor drug KRN5500. *Exp. Cell Res.* 256: 468–479
- Kistakis NT, Linder ME and Roth MG (1992) Action of brefeldin A blocked by activation of a pertussis-toxin-sensitive G protein. *Nature* 356: 344–346
- Fujii T, Garcia-Bermejo ML, Bernabo JL, Caamano J, Ohba M, Kuroki T *et al.* (2000) Involvement of protein kinase C  $\delta$  (PKC $\delta$ ) in phorbol ester-induced apoptosis in LNCaP prostate cancer cells. Lack of proteolytic cleavage of PKC $\delta$ . *J. Biol. Chem.* 275: 7574–7582
- Majumder PK, Pandey P, Sun X, Cheng K, Datta R, Saxena S *et al.* (2000) Mitochondrial translocation of protein kinase C $\delta$  in phorbol ester-induced cytochrome *c* release and apoptosis. *J. Biol. Chem.* 275: 21793–21796
- Blass M, Kronfeld I, Kazimirsy G, Blumberg PM and Brodie C (2002) Tyrosine phosphorylation of protein kinase C $\delta$  is essential for its apoptotic effect in response to etoposide. *Mol. Cell. Biol.* 22: 182–195
- Pongracz J, Webb P, Wang K, Deacon E, Lunn OJ and Lord JM (1999) Spontaneous neutrophil apoptosis involves caspase 3-mediated activation of protein kinase C-delta. *J. Biol. Chem.* 274: 37329–37334
- DeVries TA, Neville MC and Reyland ME (2002) Nuclear import of PKC $\delta$  is required for apoptosis: identification of a novel nuclear import sequence. *EMBO J.* 21: 6050–6060
- Goerke A, Sakai N, Gutjahr E, Schlapkohl WA, Mushinski JF and Haller H *et al.* (2002) Induction of apoptosis by protein kinase C delta is independent of its kinase activity. *J. Biol. Chem.* 277: 32054–32062
- Sparatore B, Patrone M, Passalacqua M, Pedrazzi M, Pontremoli S and Melloni E (2000) Human neuroblastoma cell differentiation requires protein kinase C- $\theta$ . *Biochem. Biophys. Res. Commun.* 279: 589–594
- Zeidman R, Pettersson L, Sailaja PR, Truedsson E, Fagerström S and Pählman S *et al.* (1999) Novel and classical protein kinase C isoforms have different functions in proliferation, survival and differentiation of neuroblastoma cells. *Int. J. Cancer.* 81: 494–501
- Kazanietz MG (2002) Novel 'nonkinase' phorbol ester receptors: the C1 domain connection. *Mol. Pharmacol.* 61: 759–767
- Lehel C, Olah Z, Jakab G, Anderson WB (1995) Protein kinase C  $\varepsilon$  is localized to the Golgi via its zinc-finger domain and modulates Golgi function. *Proc. Natl. Acad. Sci. USA.* 92: 1406–1410
- Singer WD, Brown HA, Jiang X and Sternweis PC (1996) Regulation of phospholipase D by protein kinase C is synergistic with ADP-ribosylation factor and independent of protein kinase activity. *J. Biol. Chem.* 271: 4504–4510
- Zeidman R, Löfgren B, Pählman S and Larsson C (1999) PKC $\varepsilon$ , via its regulatory domain and independently of its catalytic domain, induces neurite-like processes in neuroblastoma cells. *J. Cell. Biol.* 145: 713–726
- Zeidman R, Trollér U, Raghunath A, Pählman S and Larsson C (2002) Protein kinase C $\varepsilon$  actin-binding site is important for neurite outgrowth during Neuronal Differentiation. *Mol. Biol. Cell.* 13: 12–24

43. Jaken S (1996) Protein kinase C isozymes and substrates. *Curr. Opin. Cell Biol.* 8: 168–173
44. Kaufmann T, Schlipf S, Sanz J, Neubert K, Stein R and Borner C (2003) Characterization of the signal that directs Bcl-xL, but not Bcl-2, to the mitochondrial outer membrane. *J. Cell. Biol.* 160: 53–64
45. Annis MG, Zamzami N, Zhu W, Penn LZ, Kroemer G and Leber B *et al.* (2001) Endoplasmic reticulum localized Bcl-2 prevents apoptosis when redistribution of cytochrome *c* is a late event. *Oncogene* 20: 1939–1952
46. Tagami S, Eguchi Y, Kinoshita M, Takeda M and Tsujimoto Y (2000) A novel protein, RTN-XS, interacts with both Bcl-XL and Bcl-2 on endoplasmic reticulum and reduces their anti-apoptotic activity. *Oncogene* 19: 5736–5746
47. Caloca MJ, Wang H, Delemos A, Wang S and Kazanietz MG (2001) Phorbol esters and related analogs regulate the subcellular localization of beta 2-chimaerin, a non-protein kinase C phorbol ester receptor. *J. Biol. Chem.* 276: 18303–18312
48. Kashiwagi K, Shirai Y, Kuriyama M, Sakai N and Saito N (2002) Importance of C1B domain for lipid messenger-induced targeting of PKC. *J. Biol. Chem.* 277: 18037–18045
49. Maeda Y, Beznoussenko GV, Van Lint J, Mironov AA and Malhotra V (2001) Recruitment of protein kinase D to the *trans*-Golgi network via the first cysteine-rich domain. *EMBO J.* 20: 5982–5990
50. Wang H and Kazanietz MG (2002) Chimaerins, novel non-protein kinase C phorbol ester receptors, associate with Tmp21-l (p23): evidence for a novel anchoring mechanism involving the chimaerin C1 domain. *J. Biol. Chem.* 277: 4541–4550
51. Baron CL and Malhotra V (2002) Role of diacylglycerol in PKD recruitment to the TGN and protein transport to the plasma membrane. *Science* 295: 325–328
52. Mancini M, Machamer CE, Roy S, Nicholson DW, Thornberry NA and Casciola-Rosen LA *et al.* (2000) Caspase-2 is localized at the Golgi complex and cleaves golgin-160 during apoptosis. *J Cell Biol.* 149: 603–612
53. Bennett M, Macdonald K, Chan SW, Luzio JP, Simari R and Weissberg P (1998) Cell surface trafficking of Fas: a rapid mechanism of p53-mediated apoptosis. *Science* 282: 290–293
54. De Maria R, Lenti L, Malisan F, d'Agostino F, Tomassini B and Zeuner A *et al.* (1997) Requirement for GD3 ganglioside in CD95- and ceramide-induced apoptosis. *Science* 277: 1652–1655
55. Maceyka M and Machamer CE (1997) Ceramide accumulation uncovers a cycling pathway for the *cis*-Golgi network marker, infectious bronchitis virus M protein. *J. Cell Biol.* 139: 1411–1418
56. Mochly Rosen D and Gordon AS (1998) Anchoring proteins for protein kinase C: a means for isozyme selectivity. *FASEB J.* 12: 35–42
57. Hockenbery D, Nunez G, Milliman C, Schreiber RD and Korsmeyer SJ (1990) Bcl-2 is an inner mitochondrial membrane protein that blocks programmed cell death. *Nature* 348: 334–336